

# An Investigation of Plane Wave Propagation through a Layer with High Sound Speed Gradient

Alex Zinoviev, David W. Bartel and Adrian D. Jones

Maritime Operations Division, Defence Science and Technology Organisation, Edinburgh, 5111, Australia

## ABSTRACT

In modelling the reflection of sound from an ocean surface, it is necessary to include the refractive effects of near-surface bubbles generated by wind action for certain frequencies. The vertical sound speed gradient in the near-surface region is, however, so extreme that ray acoustics cannot be applied, and thus a wave approach is necessary. This paper describes the nature, and application, of a suitable wave-based description of the refraction of the intensity vector in this region of very high sound speed gradient. It is shown that the sound speed profile in the high-gradient layer can be well approximated by the sound speed profile in the "transitional" layer described by Brekhovskikh (*Waves in Layered Media*, Academic Press 1960). This exact solution of the wave equation is used to calculate the depth dependence of the acoustic pressure amplitude of the incident plane wave. The fluid particle velocity vector at the surface is also calculated and, together with the pressure amplitude, is used to obtain the intensity vector. Results show that, close to the resonance frequencies, the grazing angle at the surface is significantly larger than that predicted by the laws of geometrical acoustics. It is also shown that these resonance-like phenomena are characteristic not only of sound speed gradients typical of near-surface bubbles, but also of the less-severe gradient typical of conventional isothermal conditions.

## INTRODUCTION

It is well-known that, if the sound speed in the ocean near the surface increases with depth, a surface duct is formed where acoustic energy can be trapped. This leads to significant increase of the propagation range. Such conditions occur, for example, within an isothermal mixed layer where the sound speed increases linearly with depth due to rising hydrostatic pressure.

Sound propagation in such a layer is significantly affected by roughness of the ocean surface. The rough surface partially scatters incoming sound into different directions and, therefore, substantially increases the acoustic energy loss. As a result, any realistic model of sound propagation within the isothermal duct must take the surface roughness into consideration.

At the same time, for the evaluation of the influence of the surface roughness on reflection loss, the knowledge of the grazing angle of the acoustic wave at the surface is required. Although the grazing angle within a homogeneous isothermal layer can be evaluated without difficulties, in reality its evaluation can be significantly complicated by the presence of wind-induced bubbles near the surface, which change the compressibility of water and, as a result, the sound speed in the layer.

According to the model by Ainslie (2005), the sound speed gradients in the bubbly surface layer can be considerable. For example, at the wind speed of 10 m/s for the frequency of 2 kHz the sound speed changes by about 13 m/s within the top 3 m of the water column. Such strong gradients of the sound speed make it impossible to use the laws of ray acoustics for the purpose of calculating the grazing angle at the surface.

Therefore, the use of a wave-based theory is required for this purpose.

Jones et al. (2011) suggested a model for evaluating the loss of acoustic energy due to reflection from the rough ocean surface. The model will be called the "JBZ model" in this analysis. The results obtained by the JBZ model showed good correlation with the results obtained with the use of a Parabolic Equation transmission code.

An integral part of the JBZ model is a novel method of evaluating the grazing angle at the surface. The method is founded on a wave-based solution of the wave equation in a vertically stratified layer, which is based on a formulation provided by Brekhovskikh (1960). Although this solution has been derived by the present authors previously and utilised in Jones et al. (2011), it has not been explicitly justified in that publication.

The main purpose of this paper is to show the derivation of the wave-based solution for the acoustic wave within a layer with strong sound speed gradient, thus providing justification for one of the elements of the JBZ model. It is shown how this solution can be applied to calculate the grazing angle at the ocean surface. This solution is then used to obtain vertical acoustic pressure amplitude profiles and the differences between the grazing angles at the surface obtained using ray acoustics and the wave-based solution. In the case of the bubbly surface layer, effects at two wind speeds are considered. The calculations are also carried out for the conventional isothermal surface layer without bubbles.

The paper has the following structure. The first Section describes the method suggested by Ainslie (2005) for obtaining the sound speed profile in the bubbly layer from the wind speed above the surface. In the second Section, the formula-

tion by Brekhovskikh (1960) of an exact solution of the wave equation in a vertically stratified media is introduced. The third Section is devoted to obtaining a solution of the Helmholtz equation for the bubbly layer described by Ainslie (2005). Propagation of a plane acoustic wave through the bubbly layer and through the isothermal surface duct is considered in the fourth and the fifth Sections respectively. In the sixth Section, the assumption made by Jones et al. (2011) for determining the grazing angle at the surface in modelling practical scenarios is justified.

## INFLUENCE OF AIR BUBBLES ON SOUND SPEED IN WATER NEAR THE OCEAN SURFACE

Ainslie (2005) described the effect of wind-induced air bubbles on sound speed in the ocean. The strength of this effect is determined by the volume fraction of air near the ocean surface. It is common, for brevity, to call this parameter the “air fraction”. To determine it, Ainslie (2005) utilised a bubble population model developed by Hall (1989) and modified by Novarini (Keiffer et al. 1995). The Hall-Novarini model assumes that the radii of all bubbles lie within the interval between  $a_{\min} = 10 \mu\text{m}$  and  $a_{\max} = 1000 \mu\text{m}$ . According to this model, if the wind speed is about 10 m/s, the air fraction near the surface is about  $10^{-6}$  and quickly decreases with depth so that it becomes negligible within a few metres from the surface. Note that Ainslie’s (2005) analysis for the determination of compressibility including bubble presence did not take account of bubble resonance phenomena. That is, the compressibility was based on air fraction alone.

For calculations of the dependence of sound speed,  $c_m$ , in the mixture of water and bubbles on the vertical coordinate,  $z$ , Ainslie (2005) used the following formula:

$$c_m(z) = \frac{c_0}{\sqrt{1 + \frac{\rho_0 c_0^2}{\kappa(z) P(z)} U(z)}} \quad (1)$$

In Equation (1),  $c_0$  and  $\rho_0$  are respectively the sound speed and density in water without bubbles,  $\kappa(z)$  is the polytropic index,  $P(z)$  is the hydrostatic pressure, and  $U(z)$  is the air fraction obtained from the Hall-Novarini model. Note that, in this analysis, the vertical axis is directed downwards and, therefore,  $z$  increases with increasing depth.

Equation (1) is used to calculate the sound speed profiles shown in Figure 1 for different values of the wind speed,  $u_w$ , at

19.5 m above the ocean surface. This figure was shown originally by Jones et al. (2011).

The curves shown in Figure 1 are calculated using the following parameters:  $c_0 = 1500 \text{ m/s}$ ,  $\rho_0 = 1000 \text{ kg/m}^3$ ,  $P(z) = 101325 + 9.81z \text{ Pa}$ . The polytropic index,  $\kappa(z)$ , can vary between 1.0 and 1.4 for isothermal and adiabatic processes in gas respectively. As noted by Ainslie (2005),  $\kappa$  depends on the ratio between the bubble radius and the thermal diffusion length, which is inversely proportional to the square root of the acoustic frequency. For the bubble radii and frequencies of interest in this paper (of the order of several kHz), the process in the gas is considered to be isothermal and, therefore,  $\kappa(z) = \text{const} = 1$ .

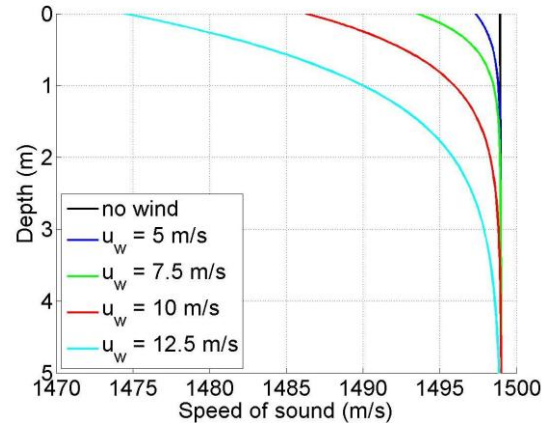


**Figure 1.** Sound speed near surface due to the effects of bubbles according to Ainslie (Equation (1)).

It is clear from Figure 1 that wind-induced bubbles near the ocean surface can lead to sound speed gradients that are much larger than the isothermal gradient of  $0.017 \text{ s}^{-1}$ . For these large gradients, for the frequency range of interest, it may be shown that the WKB approximation is not satisfied (e.g. as shown by Jones et al. (2011)). As a result, the application of ray acoustics to sound propagation in the bubbly layer cannot be justified and wave phenomena must be taken into account.

## THE EXACT SOLUTION OF THE WAVE EQUATION IN A TRANSITIONAL LAYER

This section contains Brekhovskikh’s (1960) formulation for sound propagation in a horizontally stratified layer. He showed that, for some specific sound speed profiles in the layer, the exact solution for the wave equation can be obtained analytically in closed form. He considered two types of layers. The first type is a transitional layer, where the refraction index (or sound speed) has different values at  $z = \pm\infty$ , and a symmetrical layer, where the values of the refraction index at  $z = \pm\infty$  are equal. Only the transitional layer is considered in this paper. As will be demonstrated further in this analysis, the sound speed profile of the transitional layer can be fitted to the sound speed profiles in the bubbly layer which are shown in Figure 1.

Note that Brekhovskikh (1960) considered a transitional layer where the sound speed *increases* along the direction of wave propagation. As in our case the sound speed *decreases* towards the surface, some equations are changed accordingly.

### Sound speed profile in Brekhovskikh’s transitional layer

The sound speed profile in the transitional layer is determined by the following equation:

$$c(z) = c_0 \sqrt{\frac{1-N}{1-N \frac{e^{mz}}{1+e^{mz}}}} \quad (2)$$

In Equation (2),  $m$  is a parameter,  $c_0$  is the sound speed far below the layer (i.e. at  $z=\infty$ ) without taking into consideration the isothermal gradient, and the parameter  $N$  is determined as follows:

$$N = 1 - \frac{c^2|_{z \rightarrow -\infty}}{c_0^2} = 1 - \left( \frac{2c(0) - c_0}{c_0} \right)^2 \quad (3)$$

Examples of the sound speed profiles for different values of  $m$  and  $N$  are shown in Figures 2 and 3. It is clear that  $N$  characterises the “strength” of the layer, i.e. the difference between limiting values of sound speed on both sides of the layer; and  $1/m$  characterises the thickness of the layer.

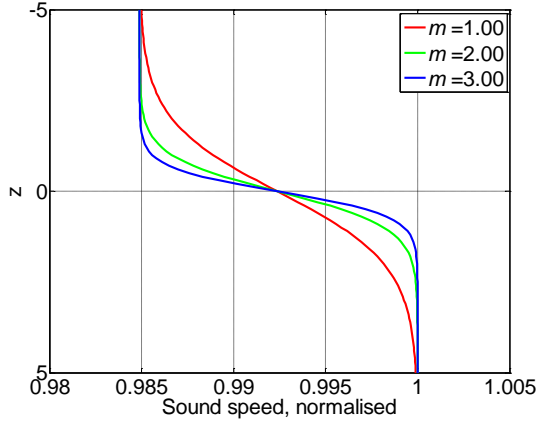


**Figure 2.** Sound speed profiles for the transitional layer for different values of  $m$ ,  $N = 0.03$ .

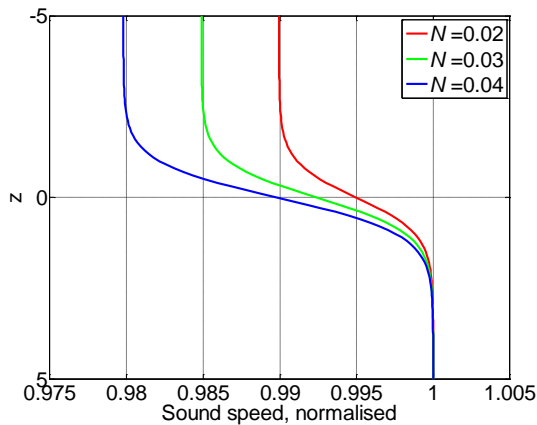


**Figure 3.** Sound speed profiles for the transitional layer for different values of  $N$ ,  $m = 2$ .

### Representation of the acoustic field in the layer

Consider a plane acoustic wave with wavevector  $\mathbf{k}_0$  approaching the layer from  $z \rightarrow \infty$ . The incident grazing angle, i.e. the angle between the wavevector and the horizontal axis at the lower boundary of the layer, is  $\theta_0$ . The propagation of such a wave through the layer is governed by the following Helmholtz equation, which is derived from the wave equation for layered-inhomogeneous media (Brekhovskikh 1960):

$$\frac{\partial^2 \psi}{\partial x^2} + \frac{\partial^2 \psi}{\partial z^2} + k^2(z)\psi = 0. \quad (4)$$

In Equation (4),  $x$  is the horizontal coordinate, and  $k(z)$  is the wavenumber depending on  $z$ . For acoustic waves,  $\psi$  is determined as follows:

$$\psi \equiv \frac{p}{\sqrt{\rho}}, \quad (5)$$

where  $p$  and  $\rho$  are the acoustic pressure and the fluid density respectively.

As the amplitude of density fluctuations in the acoustic wave is assumed to be small in comparison with the equilibrium density, the air fraction in the layer is also small (of the order of  $10^{-3}$ ), and the frequency is, in general, below the resonance frequency of the bubbles, Equation (4) can be re-written for the acoustic pressure only:

$$\frac{\partial^2 p}{\partial x^2} + \frac{\partial^2 p}{\partial z^2} + k^2(z)p = 0. \quad (6)$$

The solution of Equation (6) is sought in the form

$$p(x, z) = X(x)Z(z). \quad (7)$$

Equation (6) can be split into two equations for the two unknown functions:

$$\frac{\partial^2 Z}{\partial z^2} + [k^2(z) - a^2]Z = 0, \quad (8)$$

$$\frac{\partial^2 X}{\partial x^2} + a^2X = 0, \quad (9)$$

where  $a = k_0 \sin \theta_0$ . Based on the Equations (7), (8) and (9) the pressure field in the acoustic wave can be written as follows:

$$p(x, z) = Z(z)e^{iax}. \quad (10)$$

Therefore, to solve the problem of the plane wave propagation through the layer, it is required to find a solution  $Z(z)$  of Equation (8).

### Representation of the exact solution of the Helmholtz equation in the transitional layer via hypergeometric series

The hypergeometric equation for a function  $F(\xi)$  can be written in the form

$$\frac{d^2 F}{d\xi^2} - \frac{(\alpha + \beta + 1)\xi - \gamma}{\xi(1-\xi)} \frac{dF}{d\xi} - \frac{\alpha\beta F}{\xi(1-\xi)} = 0, \quad (11)$$

where  $\alpha$ ,  $\beta$ , and  $\gamma$  are constants.

It is noted by Brekhovskikh (1960) that, by means of some variable replacements, Equation (11) can be reduced to an equation equivalent to Equation (8). Therefore, a solution of Equation (11) is also a solution of Equation (8), i.e. it determines the vertical profile of the sound pressure in the plane wave propagating through the layer.

A solution of Equation (11) is known and can be written as the hypergeometric series:

$$F_1 = F(\alpha, \beta, \gamma, \xi) = 1 + \frac{\alpha\beta}{1 \cdot \gamma} \xi + \frac{\alpha(\alpha+1)\beta(\beta+1)}{1 \cdot 2 \cdot \gamma(\gamma+1)} \xi^2 + \dots \quad (12)$$

There exist five more solutions for Equation (11):

$$F_2 = \xi^{\gamma-1} F(\alpha - \gamma + 1, \beta - \gamma + 1, 2 - \gamma, \xi), \quad (13)$$

$$F_3 = F(\alpha, \beta, \alpha + \beta - \gamma + 1, 1 - \xi), \quad (14)$$

$$F_4 = (1 - \xi)^{\gamma - \alpha - \beta} \times \quad (15)$$

$$F(\gamma - \alpha, \gamma - \beta, \gamma - \alpha - \beta + 1, 1 - \xi),$$

$$F_5 = \xi^{-\alpha} F(\alpha, \alpha - \gamma + 1, \alpha - \beta + 1, \xi^{-1}), \quad (16)$$

$$F_6 = \xi^{-\beta} F(\beta, \beta - \gamma + 1, \beta - \alpha + 1, \xi^{-1}). \quad (17)$$

A linear combination of the functions  $F_1 \dots F_6$  is also a solution of Equation (11). The functions which need to be taken into account in the linear combination depend on the direction of acoustic wave propagation as well as on the region of convergence of each function.

For the transitional layer, the parameters of the hypergeometric series are as follows (Brekhovskikh 1960):

$$\xi = -e^{mz}, \quad (18)$$

$$\alpha = 1 + \frac{i}{2} S \left( \sin \varphi_0 - \sqrt{\sin^2 \varphi_0 - N} \right), \quad (19)$$

$$\beta = 1 + \frac{i}{2} S \left( \sin \varphi_0 + \sqrt{\sin^2 \varphi_0 - N} \right), \quad (20)$$

$$\gamma = 1 + iS \sin \varphi_0, \quad (21)$$

$$S = \frac{2k_0}{m}, \quad (22)$$

$$\cos \varphi_0 = \cos \theta_0 \sqrt{1 - N}. \quad (23)$$

The function  $Z(z)$ , which is the solution of Equation (8), can now be represented as

$$Z(z) = r_0^{-1} m^{-1/2} \xi^{1/2(\gamma-1)} (1-\xi)^{1/2(1+\alpha+\beta-\gamma)} F, \quad (24)$$

where  $r_0^{-1} = \text{const}$  and  $F$  is a linear combination of the hypergeometric functions  $F_1 \dots F_6$ .

## A SOLUTION OF THE HELMHOLTZ EQUATION IN THE TRANSITIONAL LAYER WITH DECREASING SOUND SPEED

This section describes the wave-based solution of the Helmholtz equation for the incident wave within a transitional layer with decreasing sound speed. This solution is one of the main results of this paper.

### A solution for the vertical amplitude profile

A choice of the functions  $F_1 \dots F_6$ , which need to be included into the linear combination  $F$ , can be made from the following considerations. Only region  $0 < z < \infty$  is considered here, which corresponds to  $-\infty < \xi < -1$ . It is seen from Equations (12) - (17) that only the functions  $F_5$  and  $F_6$  containing power series of  $\xi^{-1}$  converge in this region. It can be also shown that, out of these two functions, only  $F_6$  describes a wave propagating from  $z \rightarrow \infty$  to  $z = 0$ . Therefore, only the function  $F_6$  needs to be taken into account in the problem under considerations. Then the solution for the vertical profile of the acoustic pressure amplitude takes the form

$$Z(z) = (1-\xi)^{1/2(1+\alpha+\beta-\gamma)} G(\xi), \quad (25)$$

where  $G(\xi)$  is a series determined by a recurrent equation:

$$G(\xi) = \sum_{n=0}^{\infty} g_n(\xi), \quad (26)$$

$$g_0(\xi) = \xi^{-\beta+1/2(\gamma-1)}, \quad (27)$$

$$g_{n+1}(\xi) = g_n(\xi) \frac{(\beta+n)(\beta-\gamma+1+n)}{(n+1)(\beta-\alpha+1+n)} \frac{1}{\xi}. \quad (28)$$

Equations (3), (10), (18) - (23) and (25) - (28) represent the exact solution of the Helmholtz equation (6) in the transitional layer with the sound speed profile determined by Equation (2) in the half-space  $z > 0$ .

## Fitting the sound speed profile due to air bubbles to the sound speed profile in the transitional layer

It can be easily demonstrated that the sound speed profile in the bubbly layer (Equation (1)) closely resembles the sound speed profile in the transitional layer at  $z > 0$  (Equation (2)). To fit the latter profile to the former one, i.e. to choose the parameters of the transitional layer so that the two profiles are as close as possible to each other, the following procedure has been carried out.

It can be easily obtained from Equation (2) that

$$mz = \ln \left\{ \frac{\frac{c^2(z)}{c_0^2(1-N)} - 1}{1 - \frac{c^2(z)}{c_0^2}} \right\}. \quad (29)$$

It is clear that, for Brekhovskikh's transitional layer, the logarithm in the right-hand side of Equation (29) is linear with respect to depth. The closer this dependence to the linear one for any real layer with a sound speed profile, the better this layer can be described by the Brekhovskikh transitional layer.

As the series determined by Equation (28) is divergent at  $z = 0$ , it is convenient to assume that the surface of the water in Ainslie's layer does not coincide exactly with the surface  $z = 0$  in Brekhovskikh layer, but, instead, it is located at some positive depth  $z = z_0$ . Equation (29) can now be re-written and a function  $L(z)$  can be introduced as follows:

$$m(z+z_0) = \ln \left\{ \frac{\frac{c^2(z)}{c_0^2(1-N)} - 1}{1 - \frac{c^2(z)}{c_0^2}} \right\} \equiv L(z). \quad (30)$$

Requiring that the two sound speed profiles coincide at two depths,  $z_1$  and  $z_2$ , one can determine the parameters  $m$  and  $z_0$  of the Brekhovskikh's transitional layer fitted to the Ainslie's sound speed profile:

$$m = \frac{L(z_1) - L(z_2)}{z_1 - z_2}, \quad (31)$$

$$z_0 = \frac{L(z_1) - mz_1}{m}. \quad (32)$$

The depths  $z_1$  and  $z_2$  are determined by the following considerations. It is logical to assume that both profiles have the same sound speed at the surface, so that  $z_1 = 0$ . The other depth,  $z_2$ , can be chosen based on a "best fit" between the two sound speed profiles. From visual comparison of Brekhovskikh profiles obtained for different  $z_2$  with the corresponding Ainslie profile it has been concluded that the "best fit" between the two curves is achieved for  $z_2$  at which the sound speed is determined as

$$c(z_2) = c(0) + 0.72(c_0 - c(0)). \quad (33)$$

An example of the matching sound speed profiles are shown in Figure 3.

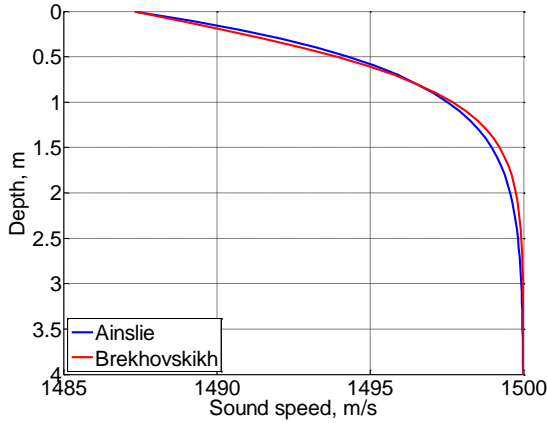


**Figure 3.** Ainslie sound speed profile due to bubbles and the matching sound speed profile in the Brekhovskikh transitional layer for wind speed  $u_w = 10$  m/s. The fitting parameters are  $m = 2.30 \text{ m}^{-1}$ ,  $z_0 = 0.0111 \text{ m}$ .

It is clear from Figure 3 that the Ainslie profile due to bubbles can be modelled well by the Brekhovskikh transitional layer.

### Grazing angle at the surface

For an acoustic wave, the energy flux vector,  $\mathbf{q}$ , is given by

$$\mathbf{q} = \frac{1}{2} \text{Re}(\mathbf{p}\mathbf{v}^*), \quad (34)$$

where  $\mathbf{v}^*$  is the complex conjugate of the fluid particle velocity vector. For a plane wave in homogeneous media, this vector is parallel to  $\mathbf{v}$  and to the wave vector,  $\mathbf{k}$ , so that the grazing angle can be determined in terms of the direction of any of these vectors.

At the same time, the bubbly layer is a medium with strong sound speed gradient where the vectors  $\mathbf{q}$ ,  $\mathbf{v}$  and  $\mathbf{k}$  may not be parallel. Therefore, the meaning of the grazing angle needs to be defined for the wave propagation in the layer. In this paper, the grazing angle is defined in terms of the direction of the energy flux vector,  $\mathbf{q}$ , which means that the grazing angle is the angle between  $\mathbf{q}$  and the horizontal axis. This definition is based upon the fact that the energy cannot penetrate the surface and, therefore, the vertical components of the energy flux vectors in the incident and the reflected waves are equal in absolute value and opposite in direction at the surface. This behaviour is analogous to behaviour of the wave vector  $\mathbf{k}$  when a plane wave is reflected by a surface in homogeneous media.

Based on the solution for the acoustic pressure in the layer obtained above, the following set of equations determining the grazing angle,  $\theta_s$ , at the surface has been derived:

$$\theta_s = \tan^{-1} \left( \frac{\text{Re}(p v_n^*)}{\text{Re}(p v_x^*)} \right), \quad (35)$$

$$v_x = \frac{a}{\omega \rho} p, \quad (36)$$

$$v_n = \frac{i}{\omega \rho} \frac{\partial p}{\partial z}, \quad (37)$$

$$\frac{\partial p}{\partial z} = \frac{\partial}{\partial z} \left( (1-\xi)^{1/2(1+\alpha+\beta-\gamma)} \right) G(\xi) + (1-\xi)^{1/2(1+\alpha+\beta-\gamma)} \frac{\partial G(\xi)}{\partial z}, \quad (38)$$

$$\frac{\partial}{\partial z} \left( (1-\xi)^{1/2(1+\alpha+\beta-\gamma)} \right) = \quad (39)$$

$$-\frac{1}{2} (1+\alpha+\beta-\gamma) (1-\xi)^{1/2(1+\alpha+\beta-\gamma)-1} m \xi,$$

$$\frac{\partial G(\xi)}{\partial z} = \sum_{n=0}^{\infty} h_n(\xi), \quad (40)$$

$$h_0(\xi) = m \left( -\beta + \frac{1}{2}(\gamma-1) \right) \xi^{-\beta+1/2(\gamma-1)}, \quad (41)$$

$$h_{n+1}(\xi) = h_n(\xi) \frac{(\beta+n)(\beta-\gamma+1+n)}{(-\beta+1/2(\gamma-1)-n)} \times \frac{(-\beta+1/2(\gamma-1)-1-n)}{(n+1)(\beta-\alpha+1+n)} \frac{1}{\xi}. \quad (42)$$

## PROPAGATION OF A PLANE WAVE THROUGH THE BUBBLY LAYER

This section deals with a plane wave propagating through the layer after having approached its lower boundary with grazing angle  $\theta_0$ . It is important to emphasize that the obtained solution of the Helmholtz equation is not its full solution, but one part of it, namely, the *incident* wave. As a result, all variability of the wave parameters across the layer is due to wave phenomena in the layer and not due to the interference of the incident and reflected waves. Obviously, the full solution can be derived by adding together the obtained solution for the incident wave and a solution for the reflected wave. Finding the latter solution is considered to be outside of the scope of this work.

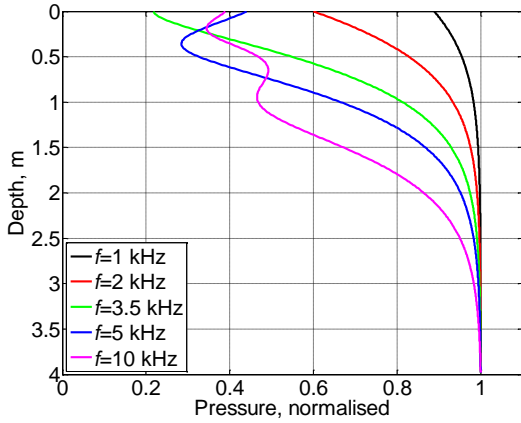
### Acoustic pressure amplitude profile

Figure 4 shows the vertical profile of the acoustic pressure amplitude in the incident wave at different frequencies. The pressure amplitude is calculated by means of Equations (25) - (28). The incident grazing angle  $\theta_0$  is equal to  $1^\circ$ , as this value is within the range of typical grazing angles for sound propagation in the surface layer (Jones et al. 2011).

It is clear from Figure 4 that wave phenomena significantly affect the pressure field in the layer. At low frequencies ( $f \leq 1$  kHz) changes in the pressure amplitude across the layer are not significant, as at these frequencies the wavelength is larger than the depth of the layer. With rising frequency, the pressure amplitude starts to decrease monotonously with decreasing depth ( $f = 2$  kHz). If the frequency rises further, minima and maxima appear in the pressure amplitude profile. For example, at  $f = 3.5$  kHz, a minimum is located close to the ocean surface and at  $f = 5$  kHz the minimum is at some distance from the surface. At a higher frequency ( $f = 10$  kHz) two minima and a maximum appear on the profile.

It may be noted that the pressure amplitude changes within the layer become much less noticeable with increasing grazing angle  $\theta_0$ . For example, for  $\theta_0 = 10^\circ$ , the normalised pressure amplitude for  $f = 3.5$  kHz at the surface is about 0.9.

Figure 5 shows the vertical profiles for the normalised pressure amplitude for wind speed  $u_w = 12.5$  m/s. It is clearly seen that, at this higher wind speed, the surface bubbly layer is deeper and the features observed in Figure 4 are more noticeable. This can be explained by higher bubble air fraction at higher wind speeds, which leads to larger changes of the sound speed within the layer and, therefore, to the stronger effect of the layer on wave propagation.



**Figure 4.** Vertical profiles of the acoustic pressure amplitude.  $\theta_0 = 1^\circ$ ,  $u_w = 10$  m/s.

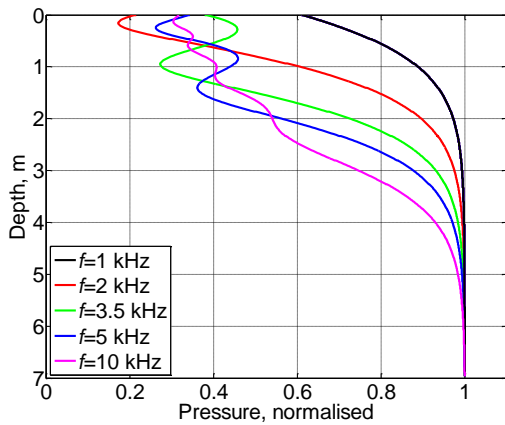


**Figure 5.** Vertical profiles of the acoustic pressure amplitude.  $\theta_0 = 1^\circ$ ,  $u_w = 12.5$  m/s.

**The grazing angle at the surface and its comparison with the grazing angle according to Snell’s law**

The influence of the wave phenomena on the sound propagation in the layer can be demonstrated by comparing the grazing angle calculated by means of the exact solution of the wave equation with the one calculated using geometrical acoustics. According to geometrical acoustics, refraction of a ray in a medium with the sound speed slowly changing along the  $z$ -axis is described by Snell’s law, which states that the following equation is satisfied along the ray path:

$$\frac{\cos \theta(z)}{c(z)} = \text{const.} \tag{43}$$

The grazing angle at the surface determined by Snell’s law,  $\theta_{sn}$ , can be found from Equation (43) as follows:

$$\cos \theta_{sn} = \frac{c(0)\cos \theta_0}{c_0}. \tag{44}$$

Figures 6 and 7 show the difference  $\theta_s - \theta_{sn}$ , where  $\theta_s$  is the grazing angle determined by the exact solution for the transitional layer (Equation (35)) at the ocean surface, in dependence on frequency and the incident grazing angle  $\theta_0$  for the wind speeds  $u_w = 10$  m/s and  $u_w = 12.5$  m/s. Colours in these Figures are selected to emphasize the areas with the positive, negative, and zero angle difference.

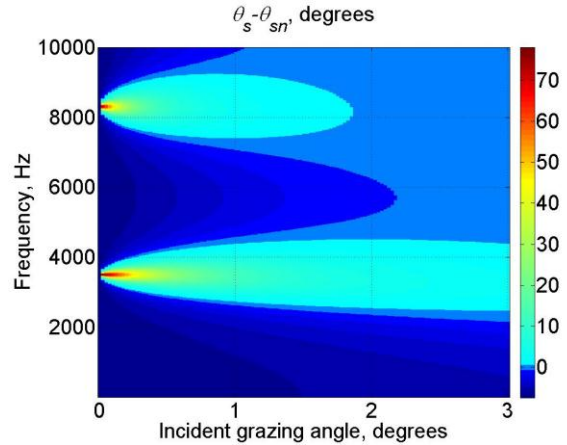


**Figure 6.** Difference between the grazing angles at the surface calculated with the use of wave-based solution and by the Snell’s law for the bubbly layer, degrees; wind speed  $u_w = 10$  m/s.

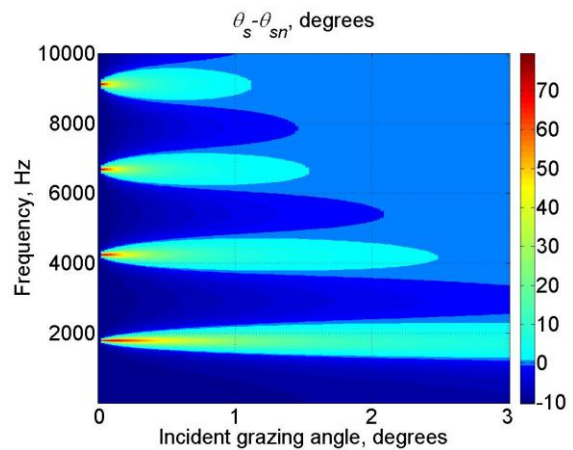


**Figure 7.** Difference between the grazing angles at the surface calculated with the use of wave-based solution and by the Snell’s law for the bubbly layer, degrees; wind speed  $u_w = 12.5$  m/s

It is clearly seen in Figures 6 and 7 that there are significant differences between the exact solution of the wave equation in the layer and the predictions of Snell’s law. The grazing angle at the surface can be either smaller or larger than that predicted by geometrical acoustics. It can be also observed that there are narrow frequency intervals where the grazing angle at the surface can reach  $70^\circ$  and more, whereas the incident grazing angle at the bottom of the layer is less than  $1^\circ$ . It means that, although the incident wave is nearly parallel to the surface, acoustic energy approaches the surface nearly normally.

These maxima in the grazing angle can be explained as modal resonances of the surface duct which exist in the bubbly layer due to its sound speed profile. The acoustic wavelength,  $\lambda_1$ , corresponding to the cut-on frequency,  $f_1$ , of the first duct mode can be found using the following equation (Urick 1983):

$$\lambda_1 = \frac{8}{3} \sqrt{2} \int_0^H \sqrt{N(z) - N(H)} dz, \tag{45}$$

where  $H$  is the thickness of the layer and  $N(z) = c_0/c(z)$  is the index of refraction.

Calculations based on Equation (45) have been conducted for the layer under considerations. Since  $c(z)$  approaches its equilibrium value  $c_0$  exponentially with increasing depth,  $H$  can take any significantly large value. In practice,  $H$  has been made equal to 10 m. The calculations show that  $f_1 = 3573$  Hz for

$u_w = 10$  m/s and  $f_1 = 1827$  Hz for  $u_w = 12.5$  m/s. Clearly, these values of  $f_1$  are very close to the frequencies of the lowest resonances in Figures 6 and 7.

It is also seen from Figures 6 and 7 that the width of the resonances along the grazing angle axis decreases with increasing frequency. This is expected, as the ray model becomes more precise at higher frequencies and, therefore, the angles obtained from both ray and wave models tend to coincide.

### PROPAGATION OF A PLANE WAVE THROUGH AN ISOTHERMAL SURFACE DUCT

It is well-known that mixed isothermal layers several tens of metres deep may exist near the ocean surface. In such a layer, the sound speed depends linearly on depth due to the influence of hydrostatic pressure. The sound speed in the layer is usually written in the form

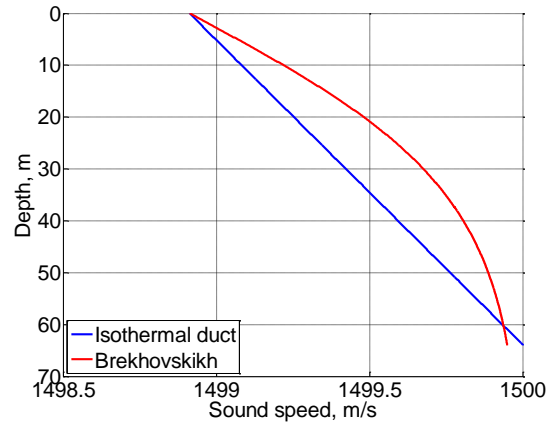
$$c(z) = c(0) + 0.017z \text{ m/s.} \quad (46)$$

In this paper, an isothermal duct of depth  $H = 64$  m is considered. The fitting parameters for the corresponding Brekhovskikh transitional layer have been chosen based on the condition of the equality of the first cut-on frequencies  $f_1$  calculated by means of Equation (45) for both layers. The resulting sound speed profiles are shown in Figure 8.

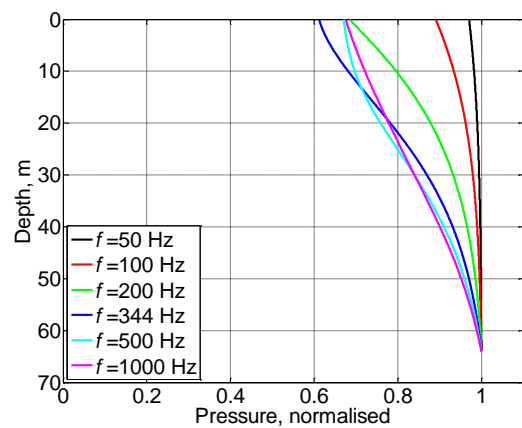
It is clear that the linear sound speed profile in the isothermal duct and the profile in the Brekhovskikh transitional layer are difficult to fit together. However, it appears to be likely that the propagation of an acoustic wave through both layers will be similar at least qualitatively as in both cases the sound speed decreases by approximately the same value along the same vertical distance.

Figure 9 shows vertical profiles of the acoustic pressure amplitude for several frequencies in the Brekhovskikh transitional layer fitted to the isothermal duct. It is clear that the pressure profiles in this layer are similar to the profiles within the bubbly layer obtained above. In both cases, the pressure decreases with decreasing depth and the minimum pressure at the surface is achieved at the first cut-on frequency, which is 344 Hz for the duct. The main difference between the two cases is that the resonance frequencies for the duct are much lower than those for the bubbly layer due to the much smaller gradient of the sound speed and larger depth in the former case.

Figure 10 is analogous to Figures 6 and 7 and shows the difference between the grazing angle at the surface obtained using the exact solution for the transitional layer and the grazing angle calculated using Snell's law. It is clearly seen that the modal resonances that correspond to the grazing angle up to tens of degrees can also be observed in the isothermal surface layer, although only for very small incident grazing angles.



**Figure 8.** Linear sound speed profile in the isothermal surface duct and the matching profile in the Brekhovskikh transitional layer,  $H = 64$  m, the fitting parameters are  $m = 0.0579 \text{ m}^{-1}$ ,  $z_0 = 0.0376 \text{ m}$ .



**Figure 9.** Vertical profiles of the acoustic pressure amplitude in the isothermal surface duct,  $H = 64$  m,  $\theta_0 = 1^\circ$ .

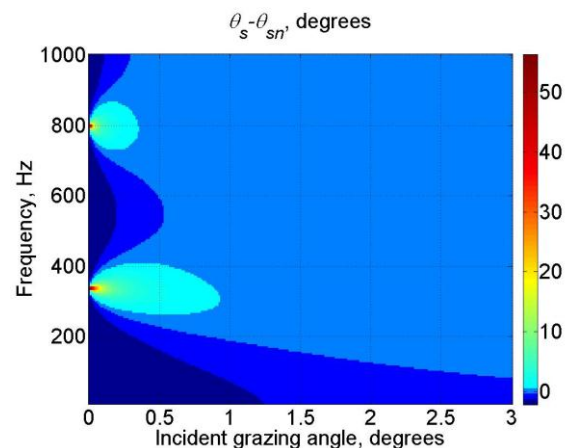


**Figure 10.** Difference between the grazing angles at the surface calculated with the use of wave-based solution and by the Snell's law for the isothermal surface duct, degrees;  $H = 64$  m.

### INFLUENCE OF THE GRAZING ANGLE AT SURFACE ON REFLECTION LOSS

The transitional layer considered in this paper is idealised in the sense that the surface of water is undisturbed. It can be assumed that the wind-induced surface roughness may lead to the conditions for the modal resonances in the duct being

disturbed and, therefore, the resonances shown in Figures 6, 7 and 10 being hard to observe. At the same time, as shown above in this analysis, wave phenomena at the surface can also lead to decrease in the grazing angle as compared with Snell's law.

The work presented in this paper shows that the grazing angle at the surface calculated using the wave-based solution can be both larger and smaller than the grazing angle due to Snell's law. For practical implementation with a ray model of transmission, Jones et al. (2011) made the assumption that the grazing angle at the surface was determined from the exact wave-based solution, unless that angle exceeded the value obtained from Snell's law. In that case it was limited to the Snell's law result, as it may be argued that the resonant phenomena, and the occurrence of very steep angles  $\theta_s$ , will not be maintained in the presence of a wind-driven moving sea surface. This method of finding the grazing angle was combined with the Small Slope Approximation surface roughness model (Williams et al. 2004) resulting in the development of the JBZ model for surface loss estimation. The results of the transmission loss calculations using the JBZ model matched well with the average transmission loss obtained by means of calculations using a Parabolic Equation transmission code for multiple realisations of the rough sea surface (Jones et al. 2011), where the latter included a sound speed variation near the surface taken from the Ainslie model.

## CONCLUSIONS

In this paper, propagation of a plane acoustic wave through a layer with a strong gradient of sound speed is considered. As an example, a layer containing wind-induced air bubbles is investigated.

It is shown that the sound speed profile within such a layer calculated with the use of the Hall-Novarini bubble population model can be closely matched by the sound speed profile within a transitional layer considered by Brekhovskikh (1960). The parameters of the transitional layer providing the best match between the two profiles are calculated.

Based on Brekhovskikh's exact solution for the transitional layer, equations determining the acoustic pressure amplitude within the layer are derived. Vertical profiles of the pressure are calculated for different frequencies. It is shown that the pressure amplitude is generally decreasing with decreasing depth, but the profiles may have maxima and minima depending on frequency.

The grazing angle at the surface derived with the use of the wave-based solution is compared with the grazing angle predicted by ray acoustics, i.e. by Snell's law. It is shown that ray acoustics can both underpredict or overpredict the grazing angle at the surface depending on the incident grazing angle and frequency.

Maxima in the grazing angle at the surface where it can reach tens of degrees, whereas the incident grazing angle is small, are exhibited. These maxima are explained via modal resonances of the acoustic duct existing in the layer due to its sound speed profile. It is shown that the frequency of the lowest observed resonance is close to the frequency of the first modal resonance calculated by means of an existing formula. It is also shown that, for a higher wind speed, the resonances appear closer to each other in frequency.

The sound speed profile in the transitional layer is also matched to the sound speed profile within an isothermal mixed layer. It is shown that the maxima in the grazing angle at the surface can also be observed in such a layer.

Finally, an assumption made by Jones et al. (2011) for the grazing angle at the surface in a layer with wind-induced bubbles and the rough surface is justified.

## REFERENCES

- Ainslie, MA 2005, 'Effect of wind-generated bubbles on fixed range acoustic attenuation in shallow water at 1-4 kHz', *J. of Acoust. Soc. Amer.*, vol. 118, no. 6, pp. 3513-23.
- Brekhovskikh, LM 1960, *Waves in layered media*, Academic Press, New York.
- Hall, MV 1989, 'A comprehensive model of wind-generated bubbles in the ocean and predictions of the effects on sound propagation at frequencies up to 40 kHz', *J. of Acoust. Soc. Amer.*, vol. 86, no. 3, pp. 1103-17.
- Jones, AD, Duncan, AJ, Bartel, DW, Zinoviev, A & Maggi, A 2011, 'Recent Developments in Modelling Acoustic Reflection Loss at the Rough Ocean Surface', *Proceedings of Acoustics 2011*, Gold Coast, Australia.
- Keiffer, RS, Novarini, JC & Norton, GV 1995, 'The impact of the background bubble layer on reverberation-derived scattering strengths in the low to moderate frequency range', *J. of Acoust. Soc. Amer.*, vol. 97, no. 1, pp. 227-34.
- Williams, KL, Thorsos, EI & Elam, WT 2004, 'Examination of coherent surface reflection coefficient (CSRC) approximations in shallow water propagation', *J. of Acoust. Soc. Amer.*, vol. 116, no. 4, pp. 1975-84.
- Urick, RJ 1983, *Principles of Underwater sound*, Peninsula Publishing, Los Altos, California.